

A Variable Structure Multirate State Estimator for Seeking Control of HDDs

Keitaro Ohno, *Member, IEEE*, and Roberto Horowitz, *Member, IEEE*

Abstract—This paper is concerned with a new multirate state estimator for the seeking control of hard disk drives (HDDs), which has a proportional, integral, and discontinuous error feedback structure to improve robustness. Conventional linear state estimators do not have sufficient accuracy under the existence of external disturbances and model uncertainty. With our proposed estimator, output-tracking performance can achieve improved robustness. Integral and discontinuous actions are introduced to alleviate the estimation error caused by disturbances and model uncertainty, while the multirate technique is used to obtain a smoother control input and higher bandwidth. Integral action and the multirate technique also alleviate the chattering caused by the discontinuous control action. Simulations and experiments have been carried out to validate our proposed multirate state estimator. Finally, an experimental implementation of proposed seeking control for single-stage and dual-stage actuated hard disk drives is demonstrated.

Index Terms—Estimator, hard disk drives (HDDs), multirate, seeking control, uncertainty, variable structure.

I. INTRODUCTION

MANY ALGORITHMS have been exploited so far for head positioning control of hard disk drives (HDDs), in order to meet the tracking requirements that are necessary to achieve increasing track densities. Among them, the multirate technique is widely used, by which we mean that, if the measurement sampling frequency is limited due to some physical condition, then, by taking a higher control input update frequency, we can achieve a smoother control input and wider control bandwidth.

Multirate control has been developed since around the late 1950s, and an early attempt for application to HDDs can be found in [1]. This idea was attractive because of its simplicity, and was extended in [2] to have a smoother intersample estimation even under the existence of external disturbances and model uncertainty. However, as we will describe in the following section, the robustness was still a key concern. More recently, multirate \mathcal{H}_∞ control design methodology for HDDs [3]–[6] has been greatly discussed to consider the robustness efficiently. In these papers, the robustness is to passively guarantee the sta-

bility in the presence of plant uncertainty, and are mostly applicable to track-following control as intended, but are not for seeking control that requires a more active approach to have the robustness.

One way to acquire such an active robustness is to apply an adaptive controller. In [8], an adaptive acceleration feedforward signal was introduced to minimize the velocity error caused by disturbances and plant parameter uncertainty during the seek. It presented actual experimental results that validate their method. These schemes usually take a certain time for adaptation to take place, so it can be said that they are primarily useful for long seeks but not for short seeks. In [7], a new way of designing a multirate feedforward seeking controller was proposed to provide perfect tracking, but little discussion was made regarding its robustness.

Another possible alternative to achieve such an active robustness is to introduce a discontinuous control action, such as sliding mode control (SMC) [9]. Several authors have tried to apply the SMC to HDDs in an attempt to alleviate the overshoot for seeking control [10]–[12], but few contributions can be found discussing its robustness. In addition, it should be pointed out that the robustness of standard SMC can only be obtained if all the states are measurable. So, if this is not the case, some modification to the estimator should be made. For this reason, the contributions so far regarding the application of SMC to HDDs are not satisfactory.

In this paper, focusing how to obtain such a robustness on an estimator design, we propose a new variable structure multirate state estimator which is based on the sliding mode observer [13] and the multirate state estimator [2]. The observer in [13] has an active robustness against parameter uncertainty, which also reduces the problem of excitation of unmodeled dynamics (spill-over problem) because there is no unmodeled dynamics in the estimator loop. The multirate estimator technique in [2] smoothes the discontinuous action and yields a smooth intersample estimation. In addition, we introduce an integral action [16], [17] to the estimation error feedback structure in order to reduce the upper bound of the uncertainty that is used to design the discontinuous action.

Our strategy toward the robust seeking control for HDDs is to improve the estimation accuracy using this proposed estimator. We will use a linear regulator in conjunction with the proposed estimator, and it achieves better robustness against uncertainty compared with a standard linear HDD seeking controller. The reason why we will not consider a discontinuous action in the regulator design is that it is not desirable to introduce a discontinuous action into the control loop since it tends to excite some unmodeled dynamics and to cause some residual vibration.

Manuscript received February 19 2003; revised February 5, 2004. Manuscript received in final form July 6, 2004. Recommended by Associate Editor D. W. Repperger. This work was conducted at the Computer Mechanics Laboratory of the University of California at Berkeley.

K. Ohno is with the Autonomous System Laboratory, Fujitsu Laboratories Limited, Atsugi, Kanagawa 243-0197, Japan (e-mail: keitaro.ohno@nifty.com).

R. Horowitz is with the Department of Mechanical Engineering, University of California at Berkeley, Berkeley, CA 94720 USA (e-mail: horowitz@me.berkeley.edu).

Digital Object Identifier 10.1109/TCST.2004.839567

In the following section, we will first review the conventional multirate estimator [2], and discuss the way of introducing the integral action. In Section III, we will introduce the variable structure to the estimator and discuss stability. In Section IV, we will concentrate on the closed-loop analysis including regulator design. In Sections V and VI, we will demonstrate how to design the proposed controller and show the simulation as well as experimental results for single and dual-stage actuated HDDs.

Throughout this paper, $\rho(\cdot)$, $\lambda(\cdot)$, $\sigma(\cdot)$, $\mathcal{R}(\cdot)$, and $\|\cdot\|$, respectively, denote the spectral radius, the eigenvalue, the singular value, range space, and Euclidian norm for vectors and spectral norm for matrices. For other notations, we will use standard mathematical expressions. Regarding the controlled plant, we considered the following multi-input–multi-output (MIMO) system so that results can be used for other applications

$$\begin{aligned}\dot{x}(t) &= Ax(t) + Bu(t) + w_c(x, u, t) \\ y(t) &= Cx(t)\end{aligned}$$

where, $x \in \mathbb{R}^n$, $y \in \mathbb{R}^p$, $u \in \mathbb{R}^m$, $A \in \mathbb{R}^{n \times n}$, $B \in \mathbb{R}^{n \times m}$, $C \in \mathbb{R}^{p \times n}$. We assume that the pair (A, B) is controllable, the pair (A, C) is observable, and B, C are both full rank. The function $w_c : \mathbb{R}^n \times \mathbb{R}^m \times \mathbb{R}_+ \mapsto \mathbb{R}^n$ represents any uncertainty. Furthermore, we assume a zeroth-order hold as the hold function and ignore time delay for simplicity. Then, the equivalent multirate system can be written as follows:

$$\begin{aligned}x(k, i+1) &= \Phi_m x(k, i) + \Gamma_m u(k, i) \\ &\quad + w(x, u, k) \\ y(k, i) &= Cx(k, 0)\end{aligned}\quad (1.1)$$

where, $\Phi_m \in \mathbb{R}^{n \times n}$ and $\Gamma_m \in \mathbb{R}^{n \times m}$ can be written as

$$\Phi_m = e^{AT_m}, \Gamma_m = \int_0^{T_m} e^{At} dt B \quad (1.2)$$

where T_m is a control update period, which is described as $T_m = T_s/r$, T_s being the measurement sampling period, and r being multirate ratio. The pair (k, i) denotes the time $t = kT_s + iT_m$, $i = 0, 1, \dots, r-1$. The function $w : \mathbb{R}^n \times \mathbb{R}^m \times \mathbb{N}_+ \mapsto \mathbb{R}^n$ represents any uncertainty that comprises an average behavior and a fluctuating behavior, each of which is, respectively, within the range space of some full rank matrices, $\Theta_B \in \mathbb{R}^{n \times q}$ and $\Theta_D \in \mathbb{R}^{n \times d}$. Thus, w can be described as follows:

$$w(x, u, k) = \Theta_B h + \Theta_D \delta h(x, u, k) \quad (1.3)$$

where $h \in \mathbb{R}^q$ and $\delta h \in \mathbb{R}^d$ are, respectively, the average and fluctuating behaviors of the uncertainty, and we assume $q \leq p$ and $d \leq p$. Also, the upper bound of δh is assumed to be known as follows:

$$\|\delta h(x, u, k)\| < h^+(x, u, k) \quad (1.4)$$

where $h^+ : \mathbb{R}^n \times \mathbb{R}^m \times \mathbb{N}_+ \mapsto \mathbb{R}_+$ is a known scalar function.

II. MULTIRATE STATE ESTIMATOR WITH I-ACTION

In this section, as preparation for the introduction of discontinuous action, integral action is introduced into a conventional

multirate state estimator so as to alleviate the detrimental effect of average behavior h of the uncertainty w in (1.3). If h can be alleviated by this I-action, it is clear that the only term that has to be dealt with by the discontinuous action becomes δh in (1.3). Thus, this leads to a significant reduction in the amount of the discontinuous feedback term that must be employed and to a reduction in the chattering problem. First, let us review the formulation of a conventional state estimator that has only a proportional feedback structure, which can be described as follows:

$$\begin{aligned}\bar{x}(k, i+1) &= \Phi_m \hat{x}(k, i) + \Gamma_m u(k, i) \\ \hat{x}(k, i) &= \bar{x}(k, i) + L_i (y(k, 0) - C\bar{x}(k, 0)) \\ \hat{e}(k, i) &= x(k, i) - \hat{x}(k, i) \\ \bar{e}(k, i) &= x(k, i) - \bar{x}(k, i)\end{aligned}$$

where \bar{x} is a prediction estimation of x , \hat{x} is a current estimation of x , and \hat{e}, \bar{e} are, respectively, the estimation error of \hat{x}, \bar{x} . $L_i \in \mathbb{R}^{n \times p}$ is a state estimation gain for i th inter sample estimation.

From the previous equation, we obtain the state estimation error dynamics, from which we can understand how w detrimentally affects the estimation accuracy

$$\bar{e}(k, i+1) = \Phi_m \bar{e}(k, i) - \Phi_m L_i C \bar{e}(k, 0) + w(x, u, k)$$

Instead of using the previous conventional estimator, the following estimator with I-action is considered, in order to alleviate the detrimental effect of h in (1.3)

$$\begin{cases} \bar{x}(k, i+1) = \Phi_m \hat{x}(k, i) + \Gamma_m u(k, i) \\ \bar{z}(k+1, 0) = \hat{z}(k, 0) \\ \hat{x}(k, i) = \bar{x}(k, i) \\ \quad + L_i \{y(k, 0) - C\bar{x}(k, 0)\} + \Theta_b \hat{z}(k, 0) \\ \hat{z}(k, 0) = \bar{z}(k, 0) + K \{y(k, 0) - C\bar{x}(k, 0)\} \end{cases} \quad (2.1)$$

where $\bar{z} \in \mathbb{R}^q$ and $\hat{z} \in \mathbb{R}^q$ are, respectively, a prediction and a current estimation of an integral state, $K \in \mathbb{R}^{q \times p}$ is a corresponding integral feedback gain, and Θ_b is a design matrix that has the same dimensions as Θ_B in (1.3).

Let us first define the following variables for simplicity:

$$\begin{aligned}\hat{e}_z(k) &:= [\hat{e}^T(k, 0) \quad \hat{z}^T(k-1, 0)]^T \\ \bar{e}_z(k) &:= [\bar{e}^T(k, 0) \quad \bar{z}^T(k, 0)]^T \\ \Psi_{\text{obs}}(i) &:= \begin{bmatrix} M(i) & N(i) \\ KC & I \end{bmatrix} \\ M(i) &:= \Phi_m^i - \sum_{j=1}^i \Phi_m^j (L_{i-j} + \Theta_b K) C \\ N(i) &:= -\Phi_m Y(i) \Theta_b \\ Y(i) &:= \sum_{j=0}^{i-1} \Phi_m^j \\ \Phi_{\text{obs}}(i) &:= \Omega^{-1} \Psi_{\text{obs}}(i) \Omega \\ &:= \begin{bmatrix} \Phi_{\text{obs}11}(i) & \Phi_{\text{obs}21}(i) \\ \Phi_{\text{obs}12} & \Phi_{\text{obs}22} \end{bmatrix} \\ \Omega &:= \begin{bmatrix} X^{-1} & X^{-1} \Theta_b \\ O & I_q \end{bmatrix} \equiv \begin{bmatrix} X & -\Theta_b \\ O & I_q \end{bmatrix}^{-1} \\ X &:= (I_n - L_0 C - \Theta_b K C)\end{aligned}\quad (2.2)$$

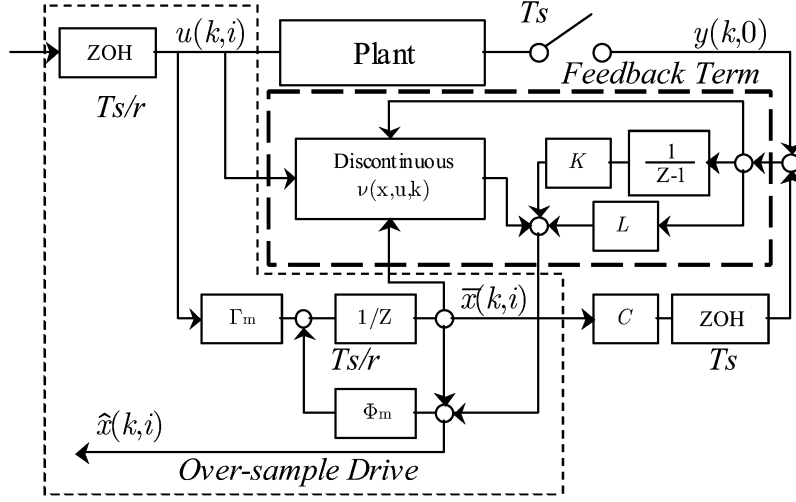


Fig. 1. Block diagram of proposed multirate estimator. Every output injection, including proportional, integral, and discontinuous action, is feedback at control update frequency.

where $\Phi_{\text{obs}} := \Phi_{\text{obs}}(r)$, $\Phi_{\text{obs}11} := \Phi_{\text{obs}11}(r) \in \mathbb{R}^{n \times n}$, $\Phi_{\text{obs}21} := \Phi_{\text{obs}21}(r) \in \mathbb{R}^{n \times q}$, $\Psi_{\text{obs}} := \Psi_{\text{obs}}(r)$, $M := M(r)$, $N := N(r)$, and $Y := Y(r)$.

For the design of linear gain matrices (K, L_i) in (2.1), we can use either dynamics of current or prediction estimation using the following result.

Lemma 1: The dynamics of the current estimation error and that of prediction estimation error for the estimator of the form in (2.1) are equivalent for the nominal linear system. In addition, the average behavior of uncertainty h in w in (1.3) can be cancelled out if $\Theta_b = \Phi_m^{-1} \Theta_B$.

Proof: See the Appendix \blacksquare

Thus, we can invoke some conventional direct pole placement techniques since the dynamics of prediction estimation can be expressed as follows, decoupling these estimation gain matrices

$$\bar{e}_z(k+1) = \begin{bmatrix} \Phi_m^r & N \\ O & I \end{bmatrix} \bar{e}_z(k) - \begin{bmatrix} \sum_{j=1}^r \Phi_m^j (L_{i-j} + \Theta_b K) \\ -K \end{bmatrix} [C \ O] \bar{e}_z(k). \quad (2.3)$$

It should be noted that we have to consider the following result for the feasibility of the pole placement.

Lemma 2: There always exists an estimator of the form in (2.1) that provides asymptotic error decay in the presence of the average behavior of the uncertainty, if and only if there is no invariant zero in the triple (Φ_m^r, N, C) at $z = 1$, and $q \leq p$.

Proof: See the Appendix. \blacksquare

As shown in [2], we may use the same proportional estimator gain for all L_i s, which can be calculated by using a single-rate estimator gain $L_{\text{sr}} \in \mathbb{R}^{n \times p}$ as follows:

$$L_{\text{mr}} (= L_0 = L_1 = \dots = L_{r-1}) + \Theta_b K = \left(\sum_{j=1}^r \Phi_m^j \right)^{-1} \Phi_m^r \cdot L_{\text{sr}}.$$

In this case, the integral gain K for both multi- and single-rate are the same. Note that it does not necessarily mean that this is the best way of selecting multirate estimator gains.

III. DISCONTINUOUS FEEDBACK

In this section, discontinuous action is introduced into the multirate estimator described in the previous section so as to alleviate the detrimental effect of the term δh in (1.3). The proposed estimator can be obtained by adding the discontinuous term to (2.1) as follows:

$$\begin{cases} \hat{x}(k, i) = \bar{x}(k, i) + L_i \{y(k, 0) - C\bar{x}(k, 0)\} \\ \quad + \Theta_b \hat{z}(k, 0) - \Theta_d \nu(k, 0) \\ \hat{z}(k, 0) = \bar{z}(k, 0) + K \{y(k, 0) - C\bar{x}(k, 0)\} \\ \nu(k, 0) = \begin{cases} -\kappa(k, x, u) \frac{DC_z \bar{e}_z(k, 0)}{\|DC_z \bar{e}_z(k, 0)\|} & \dots \text{if } DC_z \bar{e}_z \neq 0 \\ 0 & \dots \text{otherwise} \end{cases} \end{cases} \quad (3.1)$$

$$\nu(k, 0) = \begin{cases} -\kappa(k, x, u) \frac{DC_z \bar{e}_z(k, 0)}{\|DC_z \bar{e}_z(k, 0)\|} & \dots \text{if } DC_z \bar{e}_z \neq 0 \\ 0 & \dots \text{otherwise} \end{cases} \quad (3.2)$$

where $\kappa : \mathbb{N} \times \mathbb{R}^n \times \mathbb{R}^m \mapsto \mathbb{R}_+$ is a positive scalar function that satisfies $\kappa \geq h^+$, which is a design parameter, and C_z is defined as $[C \ O_{p \times q}] \in \mathbb{R}^{p \times (n+q)}$. Moreover, $D \in \mathbb{R}^{d \times p}$ is a constant matrix that must satisfy the following structural constraint:

$$C_z^T D^T = \Psi_{\text{obs}}^T P_z \Theta_z \quad (3.3)$$

where $\Theta_z^T := [(Y \Theta_D)^T \ O_{d \times q}]$, and P_z is a positive definite matrix which is a unique solution to the following Lyapunov equation:

$$\Psi_{\text{obs}}^T P_z \Psi_{\text{obs}} - P_z = -Q_z \quad (3.4)$$

where $Q_z \in \mathbb{R}^{(n+q) \times (n+q)}$ is a symmetric positive definite design matrix. The block diagram of this estimator is shown in Fig. 1. Note that the primary reason for introducing the I-action is to reduce the amount of discontinuous action. Apparently, this only works for the uncertain class given by $\{w \in \mathbb{R}^n : w \in \mathcal{R}(\Theta_B) \cap \mathcal{R}(\Theta_D)\}$.

Let us first show the following result as a preparation for establishing the stability of the proposed estimator.

Lemma 3: There exist matrices D , P_z , and Q_z that satisfy (3.3) and (3.4) only if $d \leq p$. And the fluctuation behavior δh in (1.3) can be cancelled out if $\Theta_d = \Phi_m^{-1}\Theta_D$.

Proof: From (3.3), when $d > p$, the rank of left-hand side is p while that of right-hand side is d , which means there is no positive definite solution to the Lyapunov equation, namely P_z should be zero in this case. Furthermore, the dynamics of the proposed estimator is as follows:

$$\bar{e}_z(k+1) = \Psi_{\text{obs}}\bar{e}_z(k) + Y \left\{ \begin{bmatrix} w \\ O \end{bmatrix} + \Phi_m \Theta_d \begin{bmatrix} \nu \\ O \end{bmatrix} \right\}. \quad (3.5)$$

From the second term on the right-hand side, the fluctuating behavior can be cancelled out if $\Theta_d = \Phi_m^{-1}\Theta_D$. Note that Φ_m is always nonsingular since T_m is nonzero. ■

Then, we have the following result regarding the stability.

Theorem 1: Suppose that all the conditions in Lemma 1, 2, and 3 hold, and L and K are designed such that $\rho(\Psi_{\text{obs}}) < 1$. Then there always exists an ultimately bounded sliding mode estimator. And the estimation error can be confined within the following space using $e_{zw} := [\bar{e}^T (\bar{z} - Y\Theta_B h)^T]^T$:

$$\mathcal{E}_w := \left\{ e_{zw} \in \mathbb{R}^{n+g} : \|e_{zw}\| < 2\sqrt{\frac{\lambda_{\max}(\Theta_z^T P_z \Theta_z)}{\lambda_{\min}(Q_z)}} \kappa \right\}.$$

Proof: See the Appendix. ■

Remark 1: Next, let us discuss this error space. When the uncertainty is slowly varying, this error space becomes as follows (see the Appendix for details):

$$\mathcal{E}_s := \left\{ e_{zw} \in \mathbb{R}^{n+g} : \|e_{zw}\| < \sqrt{2\frac{\lambda_{\max}(\Theta_z^T P_z \Theta_z)}{\lambda_{\min}(Q_z)}} \kappa \right\}.$$

We can see that \mathcal{E}_w is larger than \mathcal{E}_s . The physical meaning of this is that, if the uncertainty is not slowly varying, the discontinuous term may worsen the estimation error since it takes place using the information for a previous sampling time, and the discontinuous action may not work as intended. This can be easily understood by thinking of a fast varying uncertainty whose frequency is almost the same as the Nyquist frequency. Thus, for practical design, we may apply a band-limit filter to κ in (3.2), and also introduce a saturation function or other kind of function so as to alleviate the chattering. On the other hand, if no discontinuous action is applied to the estimator, the error space becomes as follows:

$$\mathcal{E}_l := \left\{ e_{zw} \in \mathbb{R}^{n+g} : \|e_{zw}\| < \left(\frac{\|\Psi_{\text{obs}}^T P_z \Theta_z\|}{\lambda_{\min}(Q_z)} + \frac{\sqrt{\|\Psi_{\text{obs}}^T P_z \Theta_z\|^2 + \lambda_{\max}(\Theta_z^T P_z \Theta_z) \lambda_{\min}(Q_z)}}{\lambda_{\min}(Q_z)} \right) h^+ \right\}.$$

From the upper-bounds of both \mathcal{E}_w and \mathcal{E}_l , we can obtain the condition such that $\mathcal{E}_w \subset \mathcal{E}_l$ as follows (see second paragraph of the Appendix for details):

$$\lambda_{\min}(Q_z) < \frac{16 \|\Psi_{\text{obs}}^T P_z \Theta_z\|^2}{9 \|\Theta_z^T P_z \Theta_z\|}. \quad (3.6)$$

See Remark 3 regarding the practical design. □

Remark 2: Moreover, as shown in [15, p. 136], “the sliding mode takes place in the error space given by $\{\bar{e}_z \in \mathbb{R}^{n+d} : DC_z \bar{e}_z = 0\}$. This does not imply $C_z \bar{e}_z = 0$ since the null space of D is nonempty and, therefore, the observer does not necessarily track the system outputs perfectly,” since we have assumed $d \leq p$. However, $C_z \bar{e}_z$ does not necessarily have to be zero by the discontinuous action since the error is bounded, as can be seen in Theorem 1. Furthermore, for a single output application, it is obvious from (3.2) that we can set $D = 1$ without loss of generality since $p = 1$ implies $d = 1$ and it follows $D \in \mathbb{R}$. In this case, the sliding mode always takes place on the error space given by $\{\bar{e}_z \in \mathbb{R}^{n+1} : C_z \bar{e}_z = 0\}$. □

Remark 3: It should also be pointed out that the solution to the structural constraint with respect to D is not easily solved, especially for a MIMO high-order system. The structural constraint for the discrete-time system shown in (3.3) is similar to those found in continuous-time variable structure realizations, which are discussed in [14] and [15]. However, each has its own difficulty as to the practical design. For example, [15] shows a way of using some coordinate transformation to represent the system in a canonical form in order to avoid this constraint problem. However, with this method, we cannot arbitrarily choose all the poles in the linear part of the estimator. Thus, it is desirable to simultaneously obtain a solution to this structural constraint along with the associated Lyapunov equation. The solution to both of these problems can be posed as a solution to the following linear matrix inequality (LMI). Note that the condition (3.6) can also be posed as a solution to an LMI and we may solve it in conjunction with the following one for practical design. □

Lemma 4: Suppose that the system matrix Ψ_{obs} in (3.3) is designed such that it is nonsingular and $\rho(\Psi_{\text{obs}}) < 1$. Then the combination of structural constraint and Lyapunov equation can be represented as the following LMI:

$$C_z^T \Lambda C_z + \Psi_{\text{obs}}^T \Theta^\perp \Upsilon \Theta^\perp \Psi_{\text{obs}} - \Psi_{\text{obs}}^{-T} C_z^T \Lambda C_z \Psi_{\text{obs}}^{-1} - \Theta^\perp \Upsilon \Theta^\perp < 0 \quad (3.7)$$

where $\Theta^\perp \in \mathbb{R}^{n \times (n+q)}$, $\Lambda \in \mathbb{R}^{p \times p}$, and $\Upsilon \in \mathbb{R}^{n \times n}$ are, respectively, the left-orthogonal complement of Θ_z , and some symmetric matrices. Moreover, we can straightforwardly design the best D for the proposed estimator by solving it along with $P_z < \gamma I$ in the minimization problem.

Proof: See the Appendix. ■

Remark 4: It is of interest to discuss the dimensional restrictions that were imposed in Lemma 2 and 3. Although we never assumed that the uncertainty must satisfy the so-called matching condition, this dimensional restriction implies that the controller cannot deal with the uncertainty when $p < m$ because a matched uncertainty means $\Theta_B = \Theta_D = \Gamma_m$, namely $q = d = m$, which apparently violates both Lemma 2 and Lemma 3.

However, this does not imply that our proposed method cannot deal with an application when $p < m$, although we have to take case-by-case analysis for each considered application. An example will follow later for dual-stage actuated HDDs where usually $p < m$. On the other hand, we can always deal with an output uncertainty as follows:

$$w = \Theta_B h + \Theta_D \delta h = T_c^{-1} \begin{bmatrix} O \\ I_p \end{bmatrix} (h + \delta h), T_c := \begin{bmatrix} N_c^T \\ C \end{bmatrix}$$

where T_c is some coordinate transformation matrix so that the output y appears in the state vector x , and N_c is an orthogonal complement of output distribution matrix C . Note that T_c is always invertible since C is full rank.

For single-stage actuated HDDs, it is straightforward to design the proposed estimator for any assumed uncertainty since it does not violate any of the dimensional constraints defined in this paper. For dual-stage actuated HDDs, it is not so straightforward to design the proposed estimator if we think of a matched uncertainty since in this case $m = q = d = 2 > p = 1$ as was mentioned earlier. However, in a practical design, we have to consider the facts that the motion range of a secondary or fine actuator [usually driven by a piezoelectric transducer (PZT)], which is mounted on the tip of a primary or coarse actuator [driven by a voice coil motor (VCM)], is physically limited, and the control bandwidth of the VCM is rather low compared with that of the PZT. This implies that the integral and discontinuous actions should not be feedback to the PZT and VCM, respectively. Thus, we should set $\Theta_B = \Gamma_{m1}$ and $\Theta_D = \Gamma_{m2}$, where Γ_{m1} and Γ_{m2} are the elements of Γ_m which, respectively, correspond to the control input of the VCM and PZT. And as we can see this arrangement does not violate any dimensional restriction. \square

IV. CLOSED-LOOP SYSTEM DESIGN

In this section, we will show how we design the closed-loop system for seeking control of HDDs. Our strategy to improve robustness is to improve the estimator's accuracy using our proposed system and to combine it with a linear regulator. Here, although we may use a conventional regulator, we introduce an alternative way to design a linear regulator, of which the idea comes from a sliding mode regulator design technique. The resulting regulator is linear in spite of the name of the design methodology, however, it still achieves better robustness against uncertainty compared with a standard HDD seek design.

A. Regulator Design

In this subsection, we will derive a linear regulator and show a practical design method. All the discussion will be for a nominal linear system. Actual closed-loop analysis will be discussed in the following subsection. First, the discrete-time switching function, $S(k, i) \in \mathbb{R}^m$, is defined with a reference input, $x_r \in \mathbb{R}^n$, as follows:

$$S(k, i) = G\{x(k, i) + x_r(k, i)\} \quad (4.1)$$

where $G \in \mathbb{R}^{m \times n}$ is a sliding hyperplane matrix. Then, the following condition is considered:

$$S(k+1) = \alpha S(k) \quad (4.2)$$

where $\alpha = \text{diag}(\alpha_1, \alpha_2, \dots, \alpha_m)$, $0 \leq \alpha_1, \alpha_2, \dots, \alpha_m < 1$. In this case, G itself does not have dynamics, but S can be thought of as having a first-order dynamics without the need to introduce any additional state as proposed in [18]. Therefore, α can be designed as follows:

$$\alpha_j = \exp(-2\pi f_j T_m) \quad (4.3)$$

where f_j denotes the cut-off frequency of j th element of switching function (or control input).

The equivalent control input can be obtained from (4.1), (4.3), and (1.1) as follows:

$$\begin{aligned} u_{\text{eq}}(k, i) &= K_{\text{eq}} \hat{x}(k, i) + x_{\text{ref}}(k, i) \\ x_{\text{ref}}(k, i) &:= -(G\Gamma_m)^{-1} \{Gx_r(k, i+1) - \alpha Gx_r(k, i)\} \\ K_{\text{eq}} &:= -(G\Gamma_m)^{-1} (G\Phi_m - \alpha G), \quad K_{\text{eq}} \in \mathbb{R}^{m \times n}. \end{aligned} \quad (4.4)$$

Note that \hat{x} is used in the previous equation. Moreover, x_{ref} can be thought of as a new reference trajectory.

Regarding the equivalent dynamics of a multirate system, substituting u in (1.1) in the expression in (4.4) as well as letting w of (1.1) and x_r of (4.4) be zero, we have the following equation:

$$\begin{aligned} x(k+1, 0) &= \Phi_{\text{eq}}^r x(k, 0) - \sum_{j=0}^{r-1} \Phi_{\text{eq}}^{r-1-j} \Gamma_m K_{\text{eq}} \hat{\ell}(k, j) \\ \Phi_{\text{eq}} &:= (\Phi_m + \Gamma_m K_{\text{eq}}), \quad \Phi_{\text{eq}} \in \mathbb{R}^{n \times n}. \end{aligned} \quad (4.5)$$

By substituting the (4.5) for the linear part of (3.5), we have

$$\begin{aligned} x(k+1, 0) &= \Phi_{\text{eq}}^r x(k, 0) \\ &\quad - \sum_{j=0}^{r-1} \Phi_{\text{eq}}^{r-1-j} \Gamma_m K_{\text{eq}} \Phi_{\text{obs11}}(j) \hat{\ell}(k, 0) \\ &\quad - \sum_{j=0}^{r-1} \Phi_{\text{eq}}^{r-1-j} \Gamma_m K_{\text{eq}} \Phi_{\text{obs12}}(j) z(k-1, 0). \end{aligned} \quad (4.6)$$

Therefore, the overall combined dynamics of the linear part of (3.5) and (4.6) can be written as follows:

$$\begin{aligned} \begin{bmatrix} \hat{e}_z(k+1) \\ x(k+1, 0) \end{bmatrix} &= \begin{bmatrix} \Phi_{\text{obs}} & O \\ E & \Phi_{\text{eq}}^r \end{bmatrix} \begin{bmatrix} \hat{e}_z(k) \\ x(k, 0) \end{bmatrix} \\ E &:= - \sum_{j=0}^{r-1} \Phi_{\text{eq}}^{r-1-j} \Gamma_m K_{\text{eq}} \begin{bmatrix} \Phi_{\text{obs11}}^T(j) \\ \Phi_{\text{obs12}}^T(j) \end{bmatrix}^T \end{aligned} \quad (4.7)$$

This eigenstructure shows that G and L can be separately designed. Note that G can be designed such that $G\Gamma$ is nonsingular

without any serious difficulty since B is full rank by assumption. Then, let us show the following result for practical design of this linear regulator.

Theorem 2: Suppose that G is designed such that $\rho(\Phi_m - \Gamma_m(G\Gamma_m)^{-1}G\Phi_m) < 1$. Then there always exists an asymptotically stable system for any choice of parameters $0 \leq \alpha_j < 1, \forall j : 1 \leq j \leq m$ such that $\rho(\Phi_{eq}) < 1$. In this case, G and α can be designed separately.

Proof: See the Appendix \blacksquare

The hyperplane matrix G can be thought of as a state feedback gain, and it can be determined in the H_2 sense in order to minimize the error from the ideal sliding hyperplane by solving a discrete algebraic Riccati equation [19]

$$\begin{aligned} \Phi_\varepsilon^T P \Phi_\varepsilon - P - \Phi_\varepsilon^T P \Gamma_m (\Gamma_m^T P \Gamma_m)^{-1} \Gamma_m^T P \Phi_\varepsilon + W &= 0 \\ G &= \Gamma_m^T P \end{aligned} \quad (4.8)$$

where P is the unique solution of (4.8), W is the weighting, and Φ_ε is a modified system matrix [20] with stability margin ε defined as follows:

$$\Phi_\varepsilon := \Phi_m + \varepsilon I, \quad 0 \leq \varepsilon < 1. \quad (4.9)$$

With this modified system matrix associated with ε , we can design G such that the spectral radius of the closed-loop system other than α be less than $1 - \varepsilon$. This implies that the cut-off frequency of associated modes can be described with ε as follows:

$$f_{co} \geq -\frac{\log_{10}(1 - \varepsilon)}{2\pi T_m}. \quad (4.10)$$

B. Closed-Loop Analysis

The complete closed-loop system dynamics including uncertainty and discontinuous action is as follows, which can be obtained in the similar manner to (4.7)

$$\begin{aligned} \begin{bmatrix} \hat{e}_z(k+1) \\ x(k+1,0) \end{bmatrix} &= \begin{bmatrix} \Phi_{obs} & O \\ E & \Phi_{eq}^r \end{bmatrix} \begin{bmatrix} \hat{e}_z(k) \\ x(k,0) \end{bmatrix} \\ &+ \begin{bmatrix} YH \\ Fw - F\{\Gamma_m K_{eq} Y(j)H\} \end{bmatrix} + \begin{bmatrix} O \\ F \end{bmatrix} x_{ref} \\ F &:= f(j) \mapsto \sum_{j=0}^{r-1} \{\Phi_{eq}^{r-1-j} f(j)\} \\ H &:= \left\{ \begin{bmatrix} w \\ O \end{bmatrix} + \Phi_m \Theta_d \begin{bmatrix} \nu \\ O \end{bmatrix} \right\} \end{aligned} \quad (4.11)$$

where x_{ref} is defined in (4.4). The second term of right-hand side of the previous equation represents the uncertainty and discontinuous action, and H can be cancelled out as we have discussed in the previous section. Thus, the problem of using the linear regulator is that we have the residual term Fw in the lower half of it.

Now, let us introduce an additional control as follows:

$$u(k) = u_{eq}(k, i) + u_{add}(k, i).$$

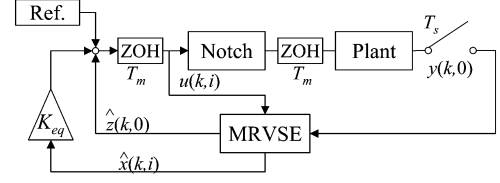


Fig. 2. Block diagram of closed-loop system. MRVSE stands for the proposed multirate variable structure estimator, and Ref. is a reference generator which corresponds to x_{ref} in (4.4).

Then, the only term that changes in (4.11) is the one discussed previously and it becomes as follows:

$$\begin{bmatrix} YH \\ F\Gamma_m u_{add} + Fw - F\{\Gamma_m K_{eq} Y(j)H\} \end{bmatrix}. \quad (4.12)$$

Since the integral and discontinuous state variables \hat{z} and ν are nothing but the estimations of average and fluctuating behaviors of uncertainty, respectively, Fw in (4.12) can be cancelled out by the selection of $u_{add} = -\nu(k,0) - \hat{z}(k,0)$ when the uncertainty satisfies the so-called matching condition, namely $\Theta_B = \Theta_D = \Gamma_m$, and we have a robust closed-loop system. However, from a practical point of view, it is again not desirable for HDDs to introduce discontinuous feedback in the control loop. Thus, we chose the following control, where u_{eq} is defined in (4.4)

$$u(k) = u_{eq}(k, i) - \hat{z}(k,0).$$

By using this logic, at the cost of less robustness in the regulator loop, we get less spill-over or residual vibration problems. The overall proposed closed-loop system is depicted in Fig. 2.

V. SEEK CONTROL FOR A SINGLE-STAGE HDD

In order to validate our proposed estimator, we demonstrate its use in the design of a seek controller for a single-stage actuated HDD, which is driven by an actuator called a VCM, and compare it with a conventional controller, of which the only difference is if there is the integral and the discontinuous action in the estimator loop and all the other parameters are the same. In other words, ν and κ in (3.1) and (3.2) are both set to zero to represent the conventional controller. The control system configuration is exactly the same as appeared in Fig. 2. Note that the measurement can be obtained by the read/write head mounted on the tip of the actuator since the position data is embedded on the magnetic disk.

A. Design Example for a Single-Stage HDD

Here, we consider a matched uncertainty, so Θ_B and Θ_D are assumed to be Γ_m . The design specifications and some of the identified parameters are shown in Table I. The experimental result of frequency response of VCM is shown in Fig. 3. Also shown in this figure is the frequency response of a mathematical model used in the simulation, whose parameters are identified by the experimental data. As a design model, we use a double

TABLE I
DRIVE SPECIFICATIONS AND IDENTIFIED PARAMETERS

Sampling freq	$1/T_s$	15kHz
Control updating freq.	$1/T_m$	45kHz
Multi-rate ratio	r	3
VCM gain	K_f	1e4
Time delay	Td	20 μ s
Track per inch	TPI	76200TPI

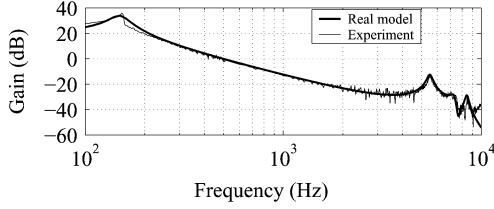


Fig. 3. Frequency characteristic of VCM. There is a large resonance mode at around 5 kHz, which will be compensated for by a series of two second-order notch filters.

integrator, and its multirate representation can be described as follows:

$$\Phi_m = \begin{bmatrix} 1 & T_m \\ 0 & 1 \end{bmatrix}, \quad \Gamma_m = K_f \begin{bmatrix} T_m^2/2 \\ T_m \end{bmatrix}, \quad C = \begin{bmatrix} 1 \\ 0 \end{bmatrix}^T.$$

For the estimator, the selection of proportional and integral gain are made so that they have characteristics of 3 kHz Butterworth and 100 Hz, respectively. The corresponding pole locations are $[0.2593+0.3192i, 0.2593-0.3192i, 0.9590]$. Utilizing Ackerman's formula [21] for direct pole placement, from (2.3) we have the estimation gain of $L_{mr} = [3.5386e-1 \ 3.3564e3]^T$ and $K = 6.0045e2$. Regarding the regulator, f in (4.3), f_{co} in (4.10), and W in (4.8) are selected as 1 kHz, 1 kHz, and $\text{diag}(1, 1)$, respectively, and we have the sliding hyperplane matrix of $G = [2.7920e4 \ 3.4652]$. To check the closed-loop characteristics for the linear part, the eigenvalues are calculated from (4.7), and we have $[0.959, 0.658, 0.584, 0.259+0.319i, 0.259-0.319i]$, which shows our desired characteristics.

Regarding the uncertainty, including nonlinearity, we consider the simple nonlinearity at control input, where the control input is equivalently to be $u_r = \text{sign}(u)\{K_g|u| + K_o\}$. u is an output of controller (command), u_r is the actual control input, K_g is the linear gain, K_o is the offset. This can be thought of as a parameter uncertainty in the input distribution matrix Γ_m and, thus, w can be modeled as follows:

$$w(k, i) = \Gamma_m \{(K_g - 1)u(k, i) \pm K_o\}. \quad (5.1)$$

From the previous w , we can easily design the discontinuous component of (3.2) as follows:

$$\nu(k, 0) = -\{K_g - 1\}_{\max}|u| + |K_o\}_{\max} \frac{C_z \bar{e}_z(k, 0)}{|C_z \bar{e}_z(k, 0)| + \delta} \quad (5.2)$$

where δ is a design parameter for a saturation function that alleviates chattering.

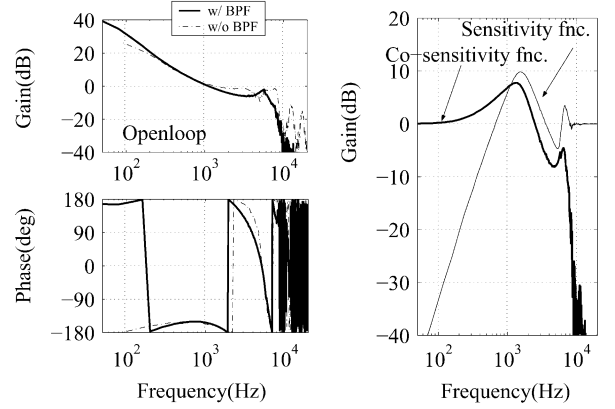


Fig. 4. Open/closed-loop characteristic (sim.) No chattering problem can be observed when a BPF is used as mentioned in Remark 1. This characteristics is quite similar to what we get for the conventional result.

B. Simulation Result for a Single-Stage HDD

Using the previous design results, we have conducted a series simulation studies. Here, we consider the parameter variation of $K_g \in [0.7, 1.3]$ and $K_o \in [-3, 3]$ (mA).

Regarding the simulation model, the controlled plant is implemented as a continuous-time system, while all the controller is as a discrete-time. Time delay is implemented by using the Padé approximation. A couple of resonant modes are compensated for by a series of two second-order notch filters. A realistic disturbance is injected, which is estimated by performing an inverse FFT to a power spectrum that was obtained by measuring a power spectrum of actual position error signal (PES) and dividing it by the measured sensitivity function.

First, the control loop frequency characteristics was checked for a nominal system. Since it is impossible to get a linearized model for a variable structure driven system, we decided to make a transfer function estimation, as follows. First, we injected some band limit white noise into the control input, then we stored the time-domain signals after and before that point. Then, by taking the cross spectrum over the power spectrum of the input signal, we can estimate the transfer function [22]. Fig. 4 shows the open-loop and closed-loop frequency characteristics as bold solid lines when we use a bandpass filter (BPF) as mentioned in Remark 1, for which we used a first-order low-pass filter whose cutoff frequency is 2 kHz. We can see there is no noticeable chattering effect due to the variable structure controller. However, without BPF, chattering occurs and it deteriorates the stability. Note that the open-loop zero crossing frequency was around 1 kHz.

Next, we conducted an output-tracking simulation study by using a sinusoidal reference input with a magnitude of one track and a frequency of 500 Hz, namely $x_r = [\sin(2\pi 500t) 0]^T$. Fig. 5 compares the results of our proposed controller against a conventional controller. The left three figures depict the references x_r , estimations \hat{x} , measurements y , and estimation errors \hat{e} for different simulation cases. The right three figures depict the corresponding current signals including command control inputs u in (5.2) and actual control inputs u_r . As can be seen from these figures, with the conventional controller, if there is an uncertainty, estimation is deteriorated, which leads to an unsatisfactory output-tracking performance, as shown in the left

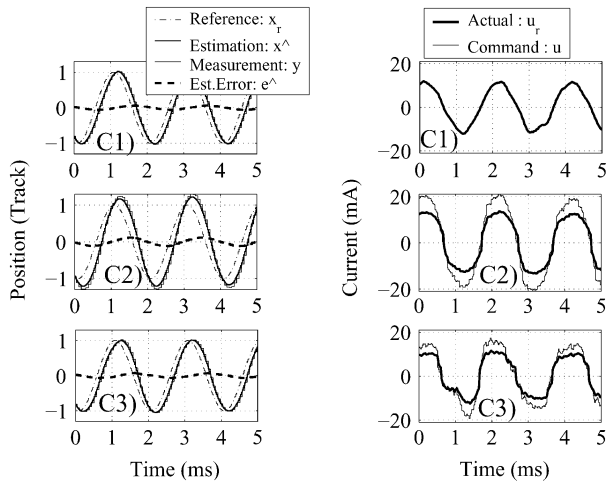


Fig. 5. Comparison of position signal (sim.) **C1**) Nominal plant w/conventional controller. **C2**) Perturbed plant w/conventional controller. **C3**) Perturbed plant w/proposed controller. Estimation of conventional controller deteriorates (middle left). Proposed estimator's performance (bottom left) is almost the same as nominal case (top left). No chattering has been observed (right).

middle figure. With our proposed controller, as shown in the left lower figure, the estimation error is almost the same as in the nominal case that is shown in the left upper figure. On the other hand, as we can see from the corresponding current signal, no detrimental effect can be seen regarding chattering of the control action.

C. Experimental Result for a Single-Stage HDD

Next, we conducted some experiments using the previously mentioned design results on a 3.5 in, 7200 rpm low profile HDD, driven by a floating point digital signal processor (DSP)(TMS320C6711) equipped with a 14-b analog to digital converter (ADC), and a 12-b digital to analog converter (DAC). The only difference between simulation and experiment regarding the system configuration is that we consider the parameter variation of $K_g \in [0.7, 1.3]$ and $K_o = 0$ (mA) since it is not easy to identify such kinds of nonlinearities with experimental setups.

In Figs. 6 and 7, we compared the 500 Hz sinusoidal response and its estimation error for different cases. From C1 to C3 cases, we can see that, with the conventional controller, the estimation error cannot be ignored when the VCM gain is decreased by 30% (C2), while our proposed controller achieved better tracking performance (C3) compared with the conventional one even under such conditions. The estimation error for the C3 case is suppressed to the same level as in the nominal case (C1). Note that each line in Fig. 7 is calculated from the difference between the thin and bold lines in Fig. 6. Moreover, from the C2 and C4 cases, with the I-action-added conventional controller, no remarkable improvement can be observed. It should be pointed out regarding the I-action that we have to consider the following three facts: 1) the uncertainty considered here lies not in h but in δh as described in (5.1); 2) the frequency of uncertainty we dealt with is 500 Hz; 3) the pole of the integral action is set to 100 Hz in order to have reasonable seeking responses and that will be described later. Furthermore, from C5 and C6

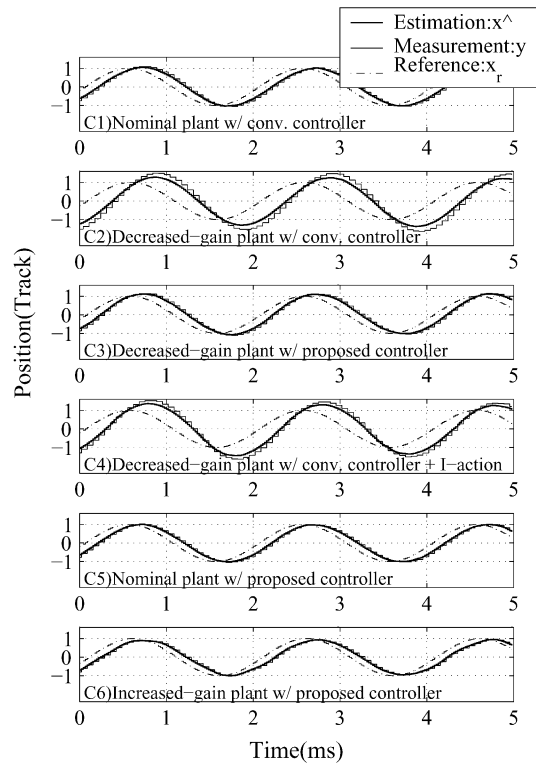


Fig. 6. Comparison of position signal (exp.).

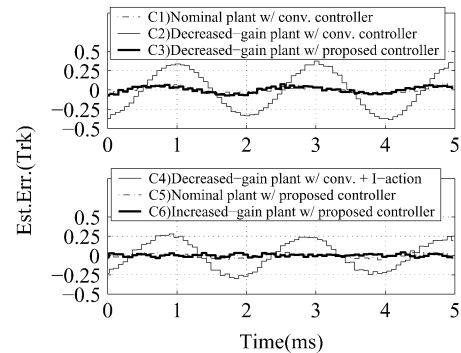


Fig. 7. Comparison of estimation error (exp.).

cases, we can see there is no detrimental effect in the use of the proposed controller for the nominal and increased-gain cases, and it works well. Note that we have also conducted some experiments for a 5 kHz response and have confirmed that there is no chattering that badly affects the response.

We then conducted an eight tracks seeking experiment on the same HDD. As a reference trajectory, the so-called minimum jerk trajectory is used [23]. Fig. 8 shows the forward and backward seeking responses (five times each) for the conventional and our proposed controllers with -30% perturbation in the VCM actuator gain. The proposed method achieves a 1 ms seek time, while the conventional controller takes almost 2.5 ms because of the presence of residual vibrations. Fig. 9 compares the corresponding estimation error. As can be seen from this figure, the estimation error of the proposed control system is much smaller than that of the conventional one, and this results in a decrease of residual vibration. Furthermore, comparing the result for nominal plant shown in Fig. 10, with that of the perturbed plant under our proposed controller, we see that the seeking

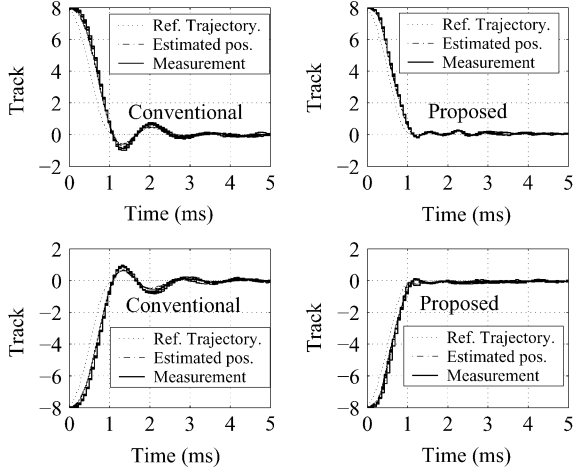


Fig. 8. Comparison of eight-track seek responses for perturbed plant. Upper two figures depict the case for forward seeking, while lower two figures depict the case for backward seeking. Conventional multirate linear controller cannot compensate for the uncertainty and, thus, we can observe some residual vibration. With proposed controller, settling time is greatly improved.

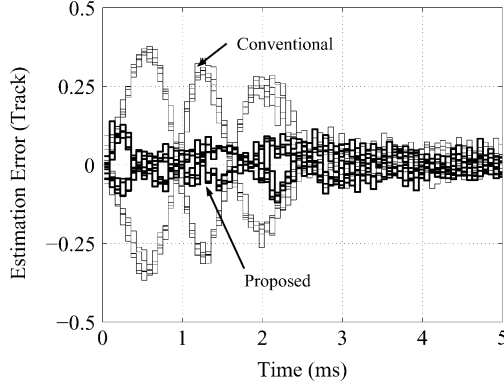


Fig. 9. Estimation error in Fig. 8. Estimation error of proposed control system is much smaller than that of conventional control system.

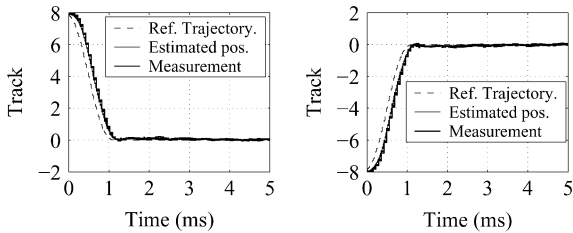


Fig. 10. Eight-track seek responses for nominal case. In comparison to Fig. 8, we can see that the settling time of proposed controller is almost the same as the nominal case.

times are almost the same. It should be note that we have the similar result in terms of improvement when the gain is increased.

VI. SEEK CONTROL OF A DUAL-STAGE HDD

Dual-stage actuated HDDs have a PZT as a fine actuator on the tip of a coarse actuator(VCM) so as to improve the positioning performance, and many control algorithms for this type of HDD have been studied, including [24]–[26] for following and [27]–[29] for seeking control.

In this section, we demonstrate the use of our proposed controller for a track-seeking control of a dual-stage actuated HDD.

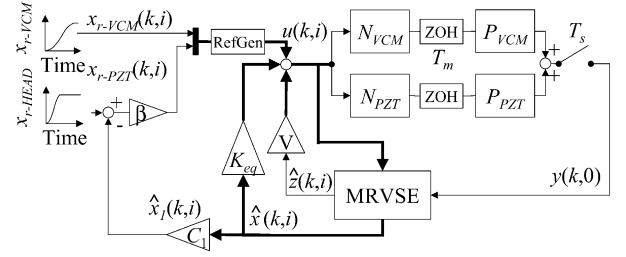


Fig. 11. Block diagram of seeking control of dual-stage actuated HDD. MRVSE stands for the proposed estimator. N_{VCM} and N_{PZT} are notch filters for VCM and PZT, respectively. V is a matrix to distribute \hat{z} to the VCM and C_1 is a conversion matrix from \hat{x} to \hat{x}_1 . Also RefGen is an operator that maps x_r to x_{ref} as described in the middle of (4.4).

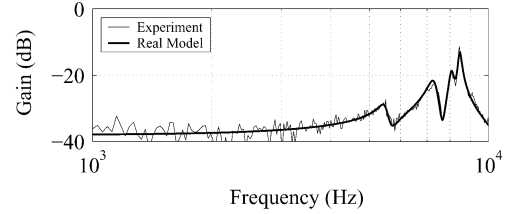


Fig. 12. Frequency characteristic of PZT. We can see several resonant modes. They are compensated for by a series of two second-order notch filters.

The specifications of the drive are the same as those shown in Table I. Fig. 12 depicts the frequency characteristics of the considered PZT actuator. Regarding the compensation for the resonant modes, we implemented a series of two second-order notch filters for the PZT actuator at 6 kHz and 8.2 kHz. Thus, the total order of the controller is 13, including four states for VCM notch filters, four states for PZT notch filters, and five states for the estimator. Fig. 11 depicts the considered control block diagram. And as a plant for design, we consider the following model for the combined system composed of VCM and PZT actuators

$$\Phi_m = \begin{bmatrix} 1 & 2.2222e-1 & 0 & 0 \\ 0 & 1 & 0 & 0 \\ 0 & 0 & 7.5129e-1 & 1.3587e-5 \\ 0 & 0 & -1.8584e4 & 2.5571e-1 \end{bmatrix}$$

$$\Gamma_m = \begin{bmatrix} 2.4691e-6 & 0 \\ 2.2222e-1 & 0 \\ 0 & 5.5089e-9 \\ 0 & 4.1164e-4 \end{bmatrix} C = \begin{bmatrix} 1 \\ 0 \\ 1 \\ 0 \end{bmatrix}^T$$

$$x =: [x_1 \ x_2 \ x_3 \ x_4]^T,$$

$$x_r =: [x_{r1} \ 0 \ x_{r3} \ 0]^T$$

where x_1, x_2, x_3, x_4 are respectively the VCM position, the VCM velocity, the PZT position, and the PZT velocity. x_{r1} and x_{r3} are respectively the reference trajectory for VCM and PZT, which are respectively designed as follows, based on the technique in [23]:

$$x_{r1} = 60y_d \left[\frac{1}{10} \left(\frac{t}{T_v} \right)^5 - \frac{1}{4} \left(\frac{t}{T_v} \right)^4 + \frac{1}{6} \left(\frac{t}{T_v} \right)^3 \right]$$

$$x_{r3} = \beta \left\{ 60y_d \left[\frac{1}{10} \left(\frac{t}{T_t} \right)^5 - \frac{1}{4} \left(\frac{t}{T_t} \right)^4 + \frac{1}{6} \left(\frac{t}{T_t} \right)^3 \right] - \hat{x}_1 \right\}$$

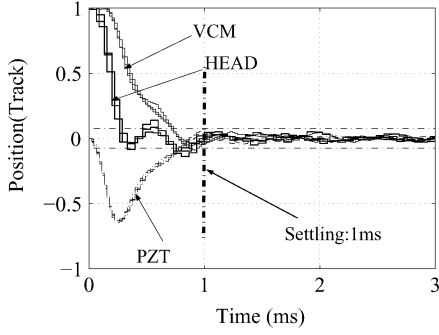


Fig. 13. Track seeking response with conventional controller for dual-stage actuated HDDs (exp.).

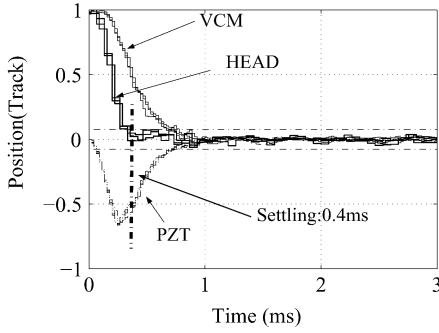


Fig. 14. Track seeking response with proposed controller for dual-stage actuated HDDs (exp.).

where T_t is the target seeking time, T_v is the target settling time for the VCM, y_d is the seeking distance, and β is a tuning parameter that is selected by a trial-and-error method.

Regarding the uncertainty, we consider the same type as considered in previous section. Thus, according to Remark 4, we have $\Theta_B = \Gamma_{m1}$ and $\Theta_D = \Gamma_{m2}$. And we consider the plant gain perturbation of 30%. The corresponding discontinuous action, thus, can be designed as follows:

$$\nu(k, 0) = -0.3|u|C_z\bar{e}_z(k, 0)/(|C_z\bar{e}_z(k, 0)| + \delta)$$

where δ is a design parameter for the saturation function that alleviates control chattering. The matrix D associated with the structural constraint in (3.3), can be set as 1, as was discussed in Remark 2 in Section III.

Regarding the linear part of the controller, with the selection of the appropriate pole location for each regulator and estimator, we have the gain of $L_{mr} = [2.4362e - 1 \ 1.5856e3 \ 1.2779e - 2 \ -2.7201e3]$, $K = 2.7890e2$, $G_{10} = [3.7168e4 \ 4.1126e0 \ 0 \ 0]$, $G_{20} = [0 \ 0 \ 1.3155e1 \ 2.0290e - 4]$, and $G = [G_{10}^T \ G_{20}^T]^T$.

Utilizing the previously mentioned design parameters, we carried out a track seeking control experiment with a dual-stage actuated HDD. Fig. 13 shows a track seeking response with a 30% PZT gain perturbation, driven by a conventional linear controller, while Fig. 14 shows the track seeking response when the system is driven by our proposed method. As can be seen from these figures, the response of the conventional controller takes a longer time to settle than our proposed method, because of the existence of residual vibration.

VII. CONCLUSION

In this paper, we have proposed a new multirate state estimator. Generally, the discontinuous action present in variable structure control systems may produce unwanted chattering. In order to avoid this problem, we have taken the following measures:

- 1) the discontinuous action takes place only in the estimator loop, which ameliorates the spill-over problem caused by unmodeled dynamics;
- 2) the introduction of a multirate system yields both smoother estimation and control action, which ameliorates undesired chattering;
- 3) the introduction of an integral action into the estimator loop decreases the magnitude of the discontinuous action, which also ameliorates undesired chattering.

We actually derived a multirate estimator that has a proportional, integral, and discontinuous error feedback structure, and have proven its stability. We also discussed how each term in the feedback structure alleviates the detrimental effect of the uncertainty. In addition, simulations were carried out for a single-stage actuated HDD, and it was confirmed that a discontinuous action can compensate for uncertainty in the actuator model. The output-tracking response for a 500 Hz-1track sinusoidal reference input with some uncertainty, driven by our proposed method, achieves almost the same performance as that for a nominal case without friction.

We also conducted a seeking control experiment on a single-stage actuated 3.5 in 7200 rpm low profile drive, and confirmed that the residual vibration caused by plant parameter uncertainty can be alleviated by the discontinuous action. The seeking time for perturbed plant was the same as that for the nominal plant.

Finally, we conducted a seeking experiment on a dual-stage actuated drive, and obtained similar results as for the single-stage actuated drive.

APPENDIX

A. Proof of Lemma 1

From (1.1) and (2.1), the prediction estimation error dynamics can be obtained as follows:

$$\bar{e}_z(k+1) = \Psi_{\text{obs}}\bar{e}_z(k) + \sum_{j=0}^{r-1} \Phi_m^j \begin{bmatrix} w \\ O \end{bmatrix}$$

and its characteristic equation for a nominal linear system can be derived as follows:

$$\det(zI - \Psi_{\text{obs}}) = 0$$

On the other hand, regarding the dynamics for current estimation error, from (2.1) and the relation $\bar{e} = \hat{e} - \bar{x} + \hat{x}$, we have the following relation:

$$\begin{aligned} \bar{e}(k, 0) &= X^{-1}\hat{e}(k, 0) + X^{-1}\Theta_b\hat{z}(k-1, 0) \\ &\Rightarrow \bar{e}_z(k) = \Omega\hat{e}_z(k) \end{aligned}$$

From previous relations, we have the dynamics for current estimation error

$$\hat{e}_z(k+1) = \Omega^{-1} \Psi_{\text{obs}} \Omega \hat{e}_z(k) + \Omega^{-1} \sum_{j=0}^{r-1} \Phi_m^j \begin{bmatrix} w \\ 0 \end{bmatrix}.$$

The characteristic equation for this dynamics is as follows:

$$\begin{aligned} \det(zI - \Phi_{\text{obs}}) \\ &= \det\{\Omega^{-1}(zI - \Psi_{\text{obs}})\Omega\} \\ &= \det(zI - \Psi_{\text{obs}}) = 0 \end{aligned}$$

Thus, both error dynamics have the same eigenvalues. Furthermore, from the first equation of this proof, the error dynamics of \bar{e} in \bar{e}_z has an I-action term given by $N\bar{z}$, which can handle the h term in w , and h is cancelled out by letting $\Theta_b = \Phi_m^{-1} \Theta_B$. Note that Φ_m is always nonsingular since T_m is nonzero in (1.2). ■

B. Proof of Lemma 2

The average behavior of the uncertainty can be dealt with if the augmented system is observable. This assures the feasibility of an arbitrary pole placement. It follows that the following pair should be observable:

$$\left(\begin{bmatrix} \Phi_m^r & N \\ O & I \end{bmatrix}, [C \quad O] \right)$$

This is equivalent to

$$\text{rank} \left(\begin{bmatrix} zI - \Phi_m^r & -N \\ O & zI - I \\ C & O \end{bmatrix} \right) = n + q \quad \forall z \in \mathbb{C}.$$

If there is an invariant zero at $z = 1$, the previous rank becomes strictly less than $n + q$. Also when $p < q$, the row rank becomes $n + p$ at $z = 1$ which is strictly less than $n + q$. Thus, there should be no invariant zero at $z = 1$ and $q \leq p$. ■

C. Proof of Theorem 1

Consider the following coordinate transformation in order to evaluate the integral state \bar{z} at the origin:

$$\bar{e}_z \mapsto e_{zw} := [\bar{e}^T \quad (\bar{z} - Y\Theta_B h)^T]^T$$

By using this coordinate transformation, (3.5) can be rewritten as follows:

$$e_{zw}(k+1) = \Psi_{\text{obs}} e_{zw}(k) + \Theta_z \delta h(k) + \Theta_z \nu(k).$$

Define the Lyapunov function candidate as follows:

$$V_{\text{obs}}(k) = e_{zw}^T P_z e_{zw}$$

where P_z is positive-definite. Evaluate the error dynamics equation along its trajectory as follows:

$$\begin{aligned} V_{\text{obs}}(k+1) - V_{\text{obs}}(k) \\ &= e_{zw}^T (\Psi_{\text{obs}}^T P_z \Psi_{\text{obs}} - P_z) e_{zw} + \delta h^T \Theta_z^T P_z \Theta_z \delta h \\ &\quad + \nu^T \Theta_z^T P_z \Theta_z \nu + 2e_{zw}^T \Psi_{\text{obs}}^T P_z \Theta_z \delta h \\ &\quad + 2e_{zw}^T \Psi_{\text{obs}}^T P_z \Theta_z \nu \\ &\quad + 2\delta h^T \Theta_z^T P_z \Theta_z \nu \end{aligned}$$

$$\begin{aligned} &\leq -e_{zw}^T Q_z e_{zw} + \|\Theta_z^T P_z \Theta_z\| (\|\delta h\|^2 + \kappa^2) \\ &\quad + 2e_{zw}^T C_z^T D^T \delta h - 2e_{zw}^T C_z^T D^T \kappa \frac{DC_z e_{zw}}{\|DC_z e_{zw}\|} \\ &\quad - 2\delta h^T \Theta_z^T P_z \Theta_z \kappa \frac{DC_z e_{zw}}{\|DC_z e_{zw}\|} \\ &\leq -\lambda_{\min}(Q_z) \|e_{zw}\|^2 + \|\Theta_z^T P_z \Theta_z\| (\|\delta h\|^2 + \kappa^2) \\ &\quad + 2\|DC_z e_{zw}\| (h^+ - \kappa) - 2\delta h^T \Theta_z^T P_z \Theta_z \kappa \frac{DC_z e_{zw}}{\|DC_z e_{zw}\|} \\ &< -\lambda_{\min}(Q_z) \|e_{zw}\|^2 + \|\Theta_z^T P_z \Theta_z\| (\|\delta h\|^2 + \kappa^2) \\ &\quad - 2\delta h^T \Theta_z^T P_z \Theta_z \kappa \frac{DC_z e_{zw}}{\|DC_z e_{zw}\|} \\ &< -\lambda_{\min}(Q_z) \|e_{zw}\|^2 + \|\Theta_z^T P_z \Theta_z\| (h^+ + \kappa)^2 \end{aligned}$$

Since Q_z is positive definite, the previous evaluation is upper convex with respect to $\|e_{zw}\|$. Thus, there always exists an ultimately bounded sliding mode estimator. The estimation error can be given by solving this equation with respect to $\|e_{zw}\|$. ■

D. Derivation of Error Space and Condition

Let us consider the special case when the sampling frequency is high enough compared to the uncertainty and the desirable error dynamics Ψ_{obs} . In such a case, the sign of each element of both $\Theta_z \delta h$ and $\Psi_{\text{obs}} e_{zw}$ can be assumed to remain the same for a few samples, since the estimation error e_{zw} caused by the uncertainty δh is $\Theta_z \delta h$ as defined in (1.3). It implies $\delta h^T \Theta_z^T \Psi_{\text{obs}} e_{zw} > 0$, which follows $\delta h^T \Theta_z^T P_z \Theta_z \Theta_z^T P_z \Psi_{\text{obs}} e_{zw} > 0 \Leftrightarrow \delta h^T \Theta_z^T P_z \Theta_z DC_z e_{zw} > 0$ by using the structural constraint in (3.3). Thus, the Lyapunov function evaluation in the Appendix becomes $V_{\text{obs}}(k+1) - V_{\text{obs}}(k) < -\lambda_{\min}(Q_z) \|e_{zw}\|^2 + \|\Theta_z^T P_z \Theta_z\| \kappa^2$, and solving it with respect to $\|e_{zw}\|$ gives the answer.

Regarding the condition (3.6), first, define positive scalars $a := \|\Psi_{\text{obs}}^T P_z \Theta_z\|$, $b := \|\Theta_z^T P_z \Theta_z\|$, and $c := \lambda_{\min}(Q_z)$. The upper-bounds for \mathcal{E}_w and \mathcal{E}_l come down to $(a + \sqrt{a^2 + bc})/c$ and $2\sqrt{bc}/c$, respectively. Take squares of both terms and subtract each other to have $(2a^2 - 3bc + 2a\sqrt{a^2 + bc})/c^2$. Concerning condition can be given by solving it such that this terms is positive.

E. Proof of Lemma 4

First, let us rewrite the constraint (3.3) as follows:

$$DC_z = \Theta_z^T P_z \Psi_{\text{obs}}$$

Note that P_z is symmetric. Then, define the following matrices, $\Theta^\dagger \in \mathbb{R}^{q \times (n+q)}$ and $\Theta^\perp \in \mathbb{R}^{n \times (n+q)}$ such that

$$T\Theta_z = \begin{bmatrix} I \\ 0 \end{bmatrix}, T := \begin{bmatrix} \Theta^\dagger \\ \Theta^\perp \end{bmatrix}.$$

Define \tilde{P}_z such that $P_z = T^T \tilde{P}_z T$, and we have

$$\begin{aligned} DC_z &= \Theta_z^T T^T \tilde{P}_z T \Psi_{\text{obs}} \\ &\Leftrightarrow DC_z \Psi_{\text{obs}}^{-1} T^{-1} = [I \quad 0] \tilde{P}_z. \end{aligned}$$

Define the following subcomponents:

$$\begin{aligned} \tilde{P}_z &= \begin{bmatrix} P_{11} & P_{12} \\ P_{12}^T & P_{22} \end{bmatrix}, \quad P_{11} \in \mathbb{R}^{q \times q}, \quad P_{22} \in \mathbb{R}^{n \times n}, \\ C_z \Psi_{\text{obs}}^{-1} T^{-1} &= [C_1 \quad C_2], \quad C_1 \in \mathbb{R}^{p \times q}, \quad C_2 \in \mathbb{R}^{p \times n}. \end{aligned}$$

Then the evaluation follows:

$$\begin{aligned} DC_z \Psi_{\text{obs}}^{-1} T^{-1} &= [I \quad 0] \tilde{P}_z \\ &\Leftrightarrow [DC_1 \quad DC_2] = [P_{11} \quad P_{12}]. \end{aligned}$$

Since P_{11} is a symmetric matrix, DC_1 is also symmetric. Thus, D can be parameterized as follows with a symmetric matrix $\Lambda \in \mathbb{R}^{p \times p}$.

$$\begin{aligned} D &= C_1^T \Lambda \\ \Rightarrow P_{11} &= DC_1 = C_1^T \Lambda C_1, \quad P_{12} = DC_2 = C_1^T \Lambda C_2 \end{aligned}$$

Then, we have

$$P_z = T^T \tilde{P}_z T = T^T \begin{bmatrix} C_1^T \Lambda C_1 & C_1^T \Lambda C_2 \\ C_2^T \Lambda C_1 & P_{22} \end{bmatrix} T.$$

Thus, P_z can be parameterized as follows:

$$P_z = \Psi_{\text{obs}}^{-T} C_z^T \Lambda C_z \Psi_{\text{obs}}^{-1} + \Theta^{\perp T} \Upsilon \Theta^{\perp}$$

where $\Upsilon \in \mathbb{R}^{n \times n}$ is a symmetric matrix. Substituting the previous equation for (3.4) gives the answer. ■

F. Proof of Theorem 2

The system can be transformed into a canonical form using the following coordinate transformation matrix:

$$T := \begin{bmatrix} I_{n-m} & O_{(n-m) \times m} \\ G_1 & G_2 \end{bmatrix}$$

where I denotes the identity matrix, and $G = [G_1 \ G_2]$. Note that the system is pretransformed into the controllable canonical form before applying T such that the system and control distribution matrix have the form

$$\Phi_{\text{eq}} =: \begin{bmatrix} \Phi_{11} & \Phi_{12} \\ \Phi_{21} & \Phi_{22} \end{bmatrix} \quad \Gamma =: \begin{bmatrix} O \\ \Gamma_2 \end{bmatrix}.$$

Then, Φ_{eq} can be transformed into

$$T \Phi_{\text{eq}} T^{-1} = \begin{bmatrix} \Phi_{11} - \Phi_{12} G_2^{-1} G_1 & \Phi_{12} G_2^{-1} \\ O & \alpha \end{bmatrix}.$$

The eigenvalues of an equivalent system matrix consist of that of $\Phi_{11} - \Phi_{12} G_2^{-1} G_1$ which is designed to be stable by the hyperplane matrix G , and α of which each element is less than one. Therefore, the equivalent system is stable for $0 \leq \alpha_j < 1$, and G and α can be designed separately. ■

REFERENCES

- [1] W.-W. Chiang, "Multirate state-space digital controller for sector servo systems," in *Proc. 29th IEEE Conf. Decision and Control*, 1990, pp. 1902–1907.
- [2] T. Hara and M. Tomizuka, "Multirate controller for hard disc drive with redesign of state estimator," in *Proc. Amer. Control Conf.*, 1998, pp. 898–903.
- [3] M. Takiguchi, M. Hirata, and K. Nonami, "Following control of hard disk drives using multi-rate H_∞ control," in *Proc. SICE Annu. Conf.*, 2002, pp. 3006–3011.
- [4] J. Ishikawa, "A study on multirate sampled-data control for hard disk drives," in *Proc. Inst. Electr. Eng. Japan Technical Meeting on Industrial Instrumentation and Control*, 2000, pp. 31–38. IIC-00-55.
- [5] T. Semba, "An H_∞ design method for a multi-rate servo controller and applications to a high density hard disk drive," in *Proc. 40th IEEE Conf. Decision and Control*, 2001, pp. 4693–4698.
- [6] K. Ohno, Y. Abe, and T. Maruyama, "Robust following control design for hard disk drives," in *Proc. IEEE Conf. Control Applications*, 2001, pp. 930–935.
- [7] H. Fujimoto, Y. Hori, T. Yamaguchi, and S. Nakagawa, "Proposal of seeking control of hard disk drives based on perfect tracking control using multirate feedforward control," in *Proc. Int. Workshop on Advanced Motion Control*, 2000, pp. 74–79.
- [8] M. Kobayashi, T. Yamaguchi, and H. Hirai, "Adaptive seeking control for magnetic disk drives," *JSME Int. J.*, vol. C-43, no. 2, pp. 300–305, 2000.
- [9] V. Utkin, J. Guldner, and J. Shi, *Sliding Mode Control in Electromechanical Systems*. New York: Taylor & Francis, 1999.
- [10] S. Lee, S. Baek, and C. Chung, "Design of a servomechanism with sliding mode for a disk drive actuator," in *Proc. IEEE 38th Conf. Decision and Control*, 1999, pp. 5253–5258.
- [11] D. Q. Zhang and G. X. Guo, "Discrete-time sliding mode proximate time optimal seek control of hard disk drives," *Proc. Inst. Electr. Eng. Control Theory and Applications*, vol. 147, no. 4, pp. 440–446, 2000.
- [12] S. Lee, S. Baek, and Y. Kim, "Design of a dual-stage actuator control system with discrete-time sliding mode for hard disk drives," in *Proc. IEEE 39th Conf. Decision and Control*, 2000, pp. 3120–3125.
- [13] B. L. Walcott and S. H. Zak, "State observation of nonlinear uncertain dynamical systems," *IEEE Trans. Autom. Control*, vol. 32, no. 2, pp. 166–170, Feb. 1987.
- [14] —, "Combined observer-controller synthesis for uncertain dynamical systems with applications," *IEEE Trans. Syst., Man, Cybern.*, vol. 18, no. 1, pp. 88–104, Jan.–Feb. 1988.
- [15] C. Edwards and S. K. Spurgeon, *Sliding Mode Control: Theory and Applications*. New York: Taylor & Francis, 1998, pp. 131–145.
- [16] S. Beale and B. Shafai, "Robust control design with a proportional integral observer," *Int. J. Control*, vol. 50, pp. 97–111, 1989.
- [17] B. Shafai and R. L. Carroll, "Design of proportional integral observer for linear time-varying multivariable systems," in *Proc. IEEE Conf. Decision and Control*, 1985, pp. 597–599.
- [18] K. D. Young and U. Ozguner, "Frequency shaped variable structure control," in *Proc. Amer. Control Conf.*, 1990, pp. 23–25.
- [19] V. I. Utkin and K. D. Young, "Methods for constructing discontinuous planes in multidimensional variable structure systems," *Autom. Remote Control*, vol. 31, pp. 1466–1470, 1977.
- [20] Y. F. Chen, H. Ikeda, T. Mita, and S. Wakui, "Trajectory control of robot arm using sliding mode control and experimented results," *J. Robotics Soc. Japan*, vol. 7, no. 6, pp. 62–67, 1989.
- [21] G. F. Franklin, J. D. Powell, and M. Workman, *Digital Control of Dynamic Systems*, 3rd ed. Reading, MA: Addison-Wesley, 1998, pp. 286–287.
- [22] P. D. Welch, "The use of fast fourier transform for the estimation of power spectra: A method based on time averaging over short, modified periodograms," *IEEE Trans. Audio Electroacoust.*, vol. AU-15, pp. 70–73, 1967.
- [23] Y. Mizoshita, S. Hasegawa, and K. Takaishi, "Vibration minimized access control for hard disk drives," *IEEE Trans. Magn.*, vol. 32, no. 3, pp. 1793–1798, May 1996.
- [24] S. Koganezawa, Y. Uematsu, T. Yamada, H. Nakano, J. Inoue, and T. Suzuki, "Dual-stage actuator system for magnetic disk drives using a shear piezoelectric microactuator," *IEEE Trans. Magn.*, vol. 35, no. 2, pp. 988–992, Mar. 1999.
- [25] D. A. Horsley, D. Hernandez, R. Horowitz, A. K. Packard, and A. P. Pisano, "Closed-loop control of a microfabricated actuator for dual-stage hard disk servo systems," in *Proc. Amer. Control Conf.*, 1998, pp. 3028–3032.
- [26] D. Hernandez, S. Park, R. Horowitz, and A. K. Packard, "Dual-stage track-following servo design for hard disk drives," in *Proc. Amer. Control Conf.*, 1999, pp. 4116–4121.
- [27] L. Guo, J. Chang, and X. Hu, "Track-following and seek/settle control for high density disk drives with dual-stage actuators," in *Proc. IEEE/ASME Int. Conf. Advanced Intelligent Mechatronics*, 2001, pp. 1136–1141.
- [28] M. Kobayashi and R. Horowitz, "Track seek control for hard disk dual-stage servo systems," *IEEE Trans. Magn.*, vol. 37, no. 2, pp. 949–954, Mar. 2001.
- [29] H. Numasato and M. Tomizuka, "Settling control and performance of dual-actuator system for hard disk drives," in *Proc. Amer. Control Conf.*, 2001.



Keitaro Ohno (M'03) was born in Tokyo, Japan, in 1968. He received the B.S. and M.S. degrees in mechanical engineering from the Tokyo Institute of Technology, Tokyo, Japan, in 1991 and 1993, respectively.

In 1993, he was with the Space Development Group, Fujitsu Limited, Atsugi, Kanagawa, Japan. In 1999, he joined the Autonomous System Laboratory in Fujitsu Laboratories Limited, working on the robust head positioning control of HDDs. From 2001 to 2003, he was a Visiting Industrial Fellow at the

Computer Mechanics Laboratory, University of California at Berkeley. He is currently with Autonomous System Laboratory, Fujitsu Laboratories Limited. His research interest includes robust and optimal control in robotics and HDD servos.

Mr. Ohno is a Member of the Society of Instrument and Control Engineers (SICE) of Japan and the American Society of Mechanical Engineers.



Roberto Horowitz (M'89) was born in Caracas, Venezuela, in 1955. He received the B.S. (with highest honors) and Ph.D. degrees in mechanical engineering from the University of California at Berkeley, in 1978 and 1983, respectively.

In 1982, he joined the Department of Mechanical Engineering, University of California at Berkeley, where he is currently a Professor. He teaches and conducts research in the areas of adaptive, learning, nonlinear, and optimal control, with applications to microelectromechanical systems (MEMS), computer

disk file systems, robotics, mechatronics, and intelligent vehicle and highway systems (IVHS).

Dr. Horowitz is a Member of the American Society of Mechanical Engineers.